ESI

Temperature dependence of the enthalpic contributions

Temperature affects lipid ordering. Generally, the higher the temperature the lower PL chain order, driven via the factor T in $F = U - T\ln\Omega$. A priori it is not clear in what way the inner energy $U(=H)$ changes with temperature. In this section we address the impact of temperature on the S-dependency of the derived interaction energy profiles. Therefore, we show the total interaction H_{tot} derived from each single temperature, shifted to 0, 20, 40, and 60 kJ/mol at S=0.35 (for 0%, 10%, 20%, and 30% CHOL respectively) to be able to clearly distinguish the temperature dependence of $H_{tot}(S)$ for each concentration (figure S1). In fact, the profiles overlap for both lipids and each respective temperature, hence the general impact on the S-dependence is weak. Only the 30% CHOL DPPC bilayer shows a slightly decreased S-dependence with temperature. Additionally, one can derive the change of free energy via the Gibbs-Helmholtz relation with

$$\frac{\partial(\beta F)}{\partial\beta} = \frac{\partial lnZ}{\partial\beta} = \frac{\left\langle He^{-\beta H}\right\rangle}{\left\langle e^{-\beta H}\right\rangle} \tag{3}$$

$$\Delta(\beta F) = \int_{\beta_1}^{\beta_3} d\beta H(\beta) = \int_{T_1}^{T_3} dT \frac{H(T)}{k_{\mathrm{B}}T^2} \tag{4}$$

$$\Rightarrow \Delta(\beta F) \approx \frac{\Delta T}{6k_{\mathrm{B}}}\left(\frac{H(T_1)}{T_1^2} + \frac{4H(T_2)}{T_2^2} + \frac{H(T_3)}{T_3^2}\right) \tag{5}$$

where β is the inverse product of the molar gas constant R and the temperature T and Z being the partition function. For the estimation of the intergral in eq. 5 we have used the Simpson's rule. Analogous to equation 1 one can expand the relation in eq. 3 to terms depending on order, e.g. $F(S)$ and $H(S)$. We used 290, 300 and 310 K (DLiPC) and 330, 340 and 350 K (DPPC) for T_1, T_2 and T_3 respectively to compute the change of $F(S)$ with temperature. The results are shown in figure S2. As expected from the results of figure S1, the computed free energy change is only weekly depending on PL order. The absolute change is higher in the case of DLiPC though. Moreover, the results show, that the temperature effect is similar for all CHOL concentrations.

In summary, the discussed results show that the S-dependence of the derived energy profiles $H(T,S)$ is not affected by temperature effects and, surprisingly, the $\Delta(\beta F)$ profiles are similar for all CHOL concentrations.

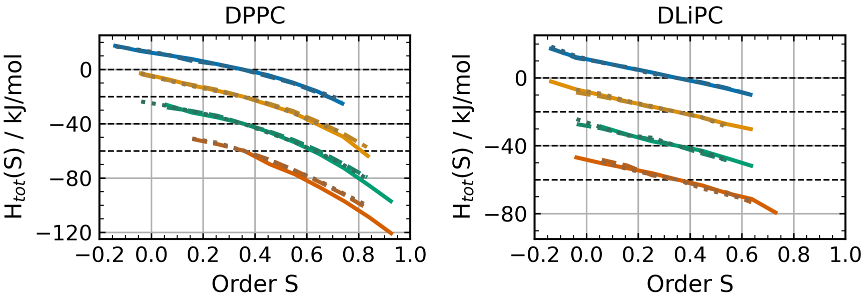

Fig. S1 Total interaction energy of a PL with its surrounding as a function of the PL order parameter at different concentrations (0%, blue; 10%, yellow, 20% green, 30%, red) and temperatures (290 K, 310 K, 330 K for DLiPC and 330 K to 350 K for DPPC; in solid, dashed and dotted respectively). The functions where shifted to 0, 20, 40 and 60 kJ/mol (black dashed lines) at S=0.35 to be able to clearly distinguish between the concentrations and to make temperature effects clearly visible.

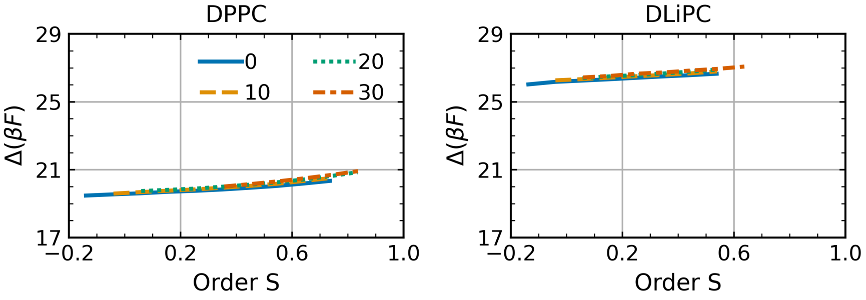

Fig. S2 Change of the ratio of free energy and thermal energy as a function of the order parameter at CHOL concentrations of 0% to 30%.

Additional data

Table S1 Parameters of the MD simulations.

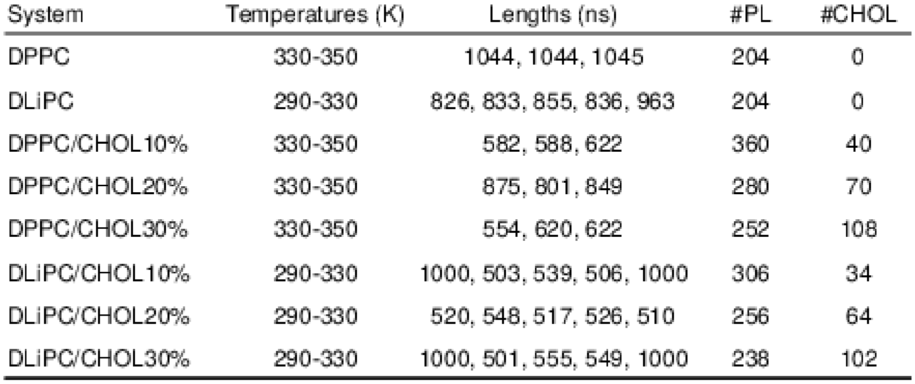

System	Temperatures (K)	Lengths (ns)	#PL	#CHOL
DPPC	330-350	1044, 1044, 1045	204	0
DLiPC	290-330	826, 833, 855, 836, 963	204	0
DPPC/CHOL10%	330-350	582, 588, 622	360	40
DPPC/CHOL20%	330-350	875, 801, 849	280	70
DPPC/CHOL30%	330-350	554, 620, 622	252	108
DLiPC/CHOL10%	290-330	1000, 503, 539, 506, 1000	306	34
DLiPC/CHOL20%	290-330	520, 548, 517, 526, 510	256	64
DLiPC/CHOL30%	290-330	1000, 501, 555, 549, 1000	238	102

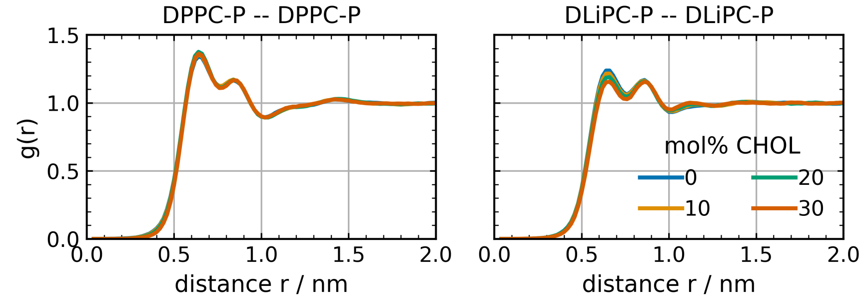

Fig. S3 Radial distribution functions of the lateral distances between P atoms. The RDFs were calculated individually for each leaflet and averaged over.

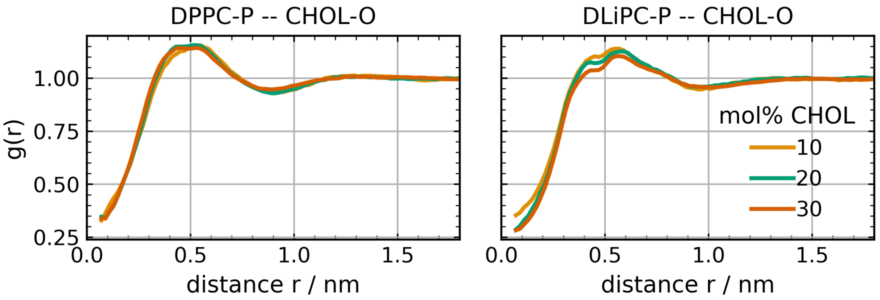

Fig. S4 Radial distribution functions of the lateral distances between P and O atoms. The RDFs were calculated individually for each leaflet and averaged over.

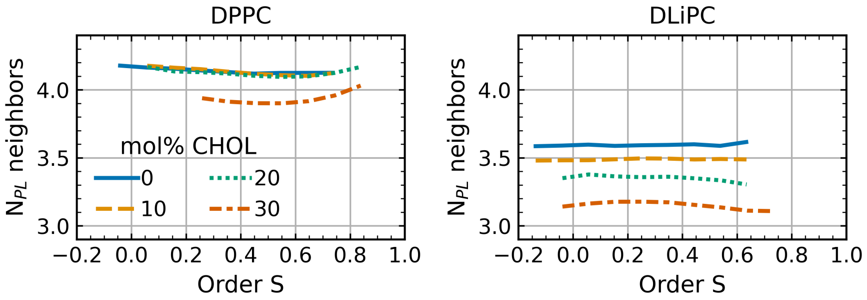

Fig. S5 Average number of nearest PL neighbors of DPPC (left) and DLiPC (right) as a function of the lipid's order parameter.

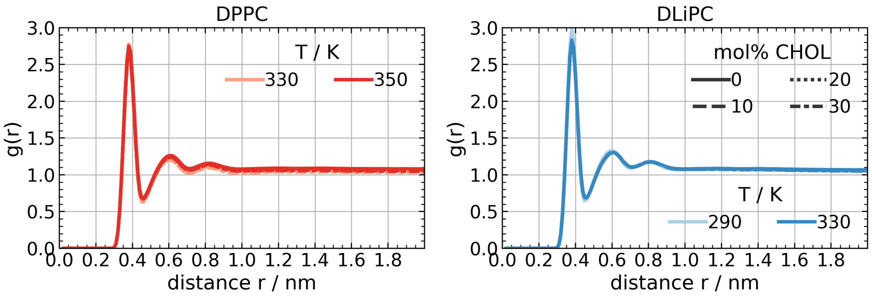

Fig. S6 Radial distribution functions of the distances between PL phosphor atoms and oxygen atoms of water.

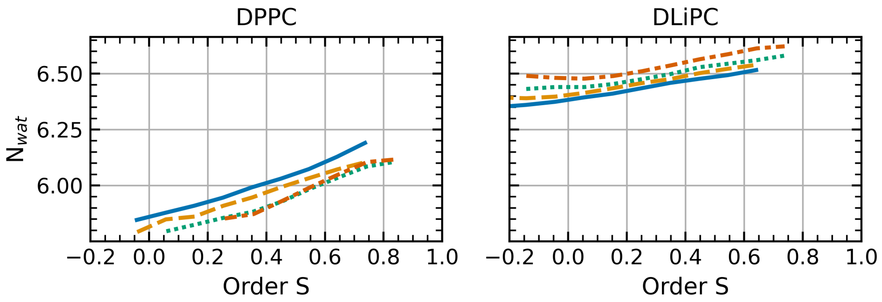

Fig. S7 Average number of water molecules around PL phosphor atoms as a function of the PL chain order parameter. Solid blue, dashed yellow, dotted green, and dot-dashed red indicate that energies were derived from bilayers with CHOL concentrations of 0, 10, 20 and 30 mol% respectively.

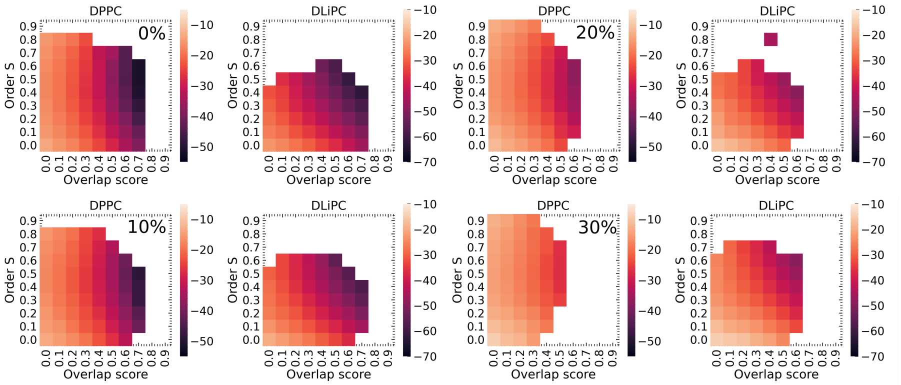

Fig. S8 Interleaflet interaction as a function of both, the lipids overlap and its chain order parameter in respective bilayer DPPC/CHOL and DLiPC/CHOL mixtures from 0% to 30% CHOL.

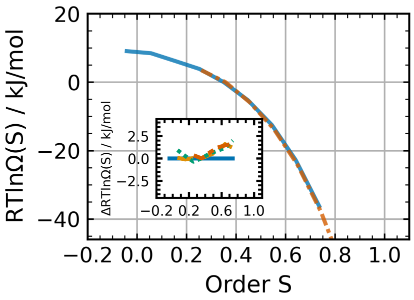

Fig. S9 Estimation of the acyl chain entropy of DPPC derived from the total sum of all enthalpic energy contributions and the order parameter distributions in the simulations at two CHOL concentrations and the difference between the respective estimates in bilayer composition from 0% to 30% CHOL (inset). Solid blue, dashed yellow, dotted green, and dot-dashed red indicate that energies were derived from bilayers with CHOL concentrations of 0, 10, 20, and 30 mol% respectively.

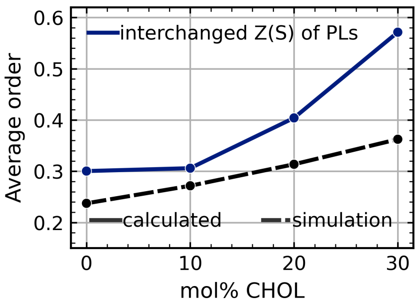

Fig. S10 Average order parameter of DLiPC in a bilayer simulation at 330 K (dashed) as a function of CHOL concentration, and the recalculated average order parameter when the $H_{DPPC}(S)$ is used along with $Z_{DLiPC}(S)$ (solid).